Quantitative WB-MRI with ADC Histogram Analysis for Complex Response of Bone Marrow Metastatic Disease

Danoob Dalili[1]; Anwar R. Padhani[2]; Robert Grimm[3]

[1] Imperial College Healthcare NHS Trust, St Mary's Hospital, London, United Kingdom
[2] Paul Strickland Scanner Centre, Mount Vernon Cancer Centre, Northwood, Middlesex, United Kingdom
[3] Siemens Healthineers, Erlangen, Germany

Introduction

Bone metastases and bone specific malignancies such as multiple myeloma, remain diagnostically challenging not only for disease detection, but also when monitoring disease response to treatments. Recently, whole-body MRI (WB-MRI) incorporating diffusion sequences has been shown to be able to potentially advance the care of breast and prostate cancer patients who have a high metastatic bone disease prevalence, by improving disease detection [1, 2]. In 2015, WB-MRI was accepted into patient care guidelines by the International Myeloma Working Group [3] for disease detection and prognostication.

The incorporation of diffusion imaging sequences into WB-MRI protocols has been shown to improve both bone disease detection and response assessments. WB-MRI with diffusion sequences has the potential to alter clinical diagnostic thinking when assessing bone disease response. This is because it becomes possible to positively assess the success of therapy benefit in diseased bone, which is not possible when using CT and bone scans. Imaging standards for the conduct and systematic reporting of WB-MRI, including therapy response criteria were recently published [4].

Figure 1: Morphological images and high b-value DWI, maximum intensity projections (MIPs).

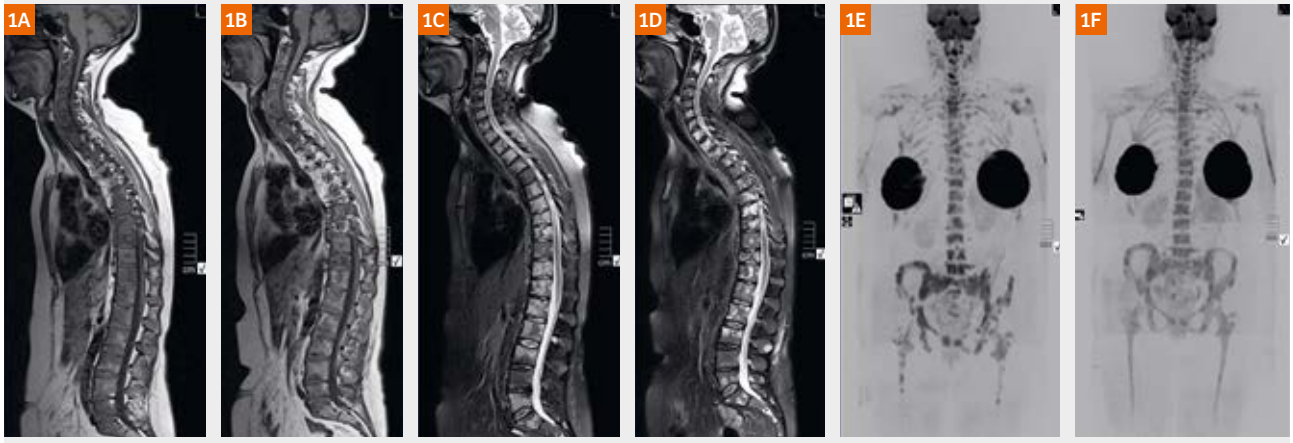

Left 2-columns **(1A, 1B)**: Whole-spine sagittal T1-weighted images show diffuse bone marrow infiltration (1A) with some return of bone marrow fat after chemotherapy (1B).

Middle 2-columns **(1C, 1D)**: Whole-spine sagittal T2w-fs sequences show diffuse bone marrow infiltration (1C) with subtle increases in signal intensity following chemotherapy (1D). The increases in T2w bone marrow signal intensity after therapy are consistent with alternations in tissue water content which is associated with tumor cell kill.

Right 2-columns **(1E, 1F)**: Whole-body b900 3D MIP (inverted scale). The bone marrow is diffusely involved with diffuse regions of high signal intensity in the axial skeleton and in the proximal limb bones before therapy (1E). A global reduction in the b900 signal intensity of bone marrow can be seen, consistent with disease response (1F). There is also uniform increase in extent of signal in the limbs consistent with bone marrow regeneration. Bilateral breast prostheses are also visible.

Uniquely, diffusion imaging brings a degree of objectivity to response assessments, using quantitative apparent diffusion coefficient measurements (ADC; unit $\mu m^2/s$). ADC maps of whole-body disease load, allow objective assessments of bone tumor load and therapy response [5]. There is a high inter and intra-observer agreement of whole-body ADC mapping [6]. Semi-automated threshold-based, quantitative ADC mapping and histogram analysis software, allow deployment of whole-body ADC mapping into the clinic [7].

There is a need for radiologists to understand the biological meaning and likely clinical implications of changes observed in quantitative whole-body ADC maps and histograms. This is particularly the case for malignant bone disease, where diffusion signal changes can arise from the normal bone marrow as well as from malignant tissues, both of which can be intermixed. Several articles have been published in MAGNETOM Flash illustrating the ADC back-mapping technique [7, 8] and tumor therapy response applications [8]. These illustrations have noted that ADC changes reflect on the mechanism of tumor cell death and the re-emergence of tumor cells when therapy resistance arises. In this case report, we demonstrate the ability of the whole-body tumor load software to distinguish ADC changes ascribable to tumor response and bone marrow recovery with successful therapy. Longer-term changes are described in a companion case [9] in this issue of MAGNETOM Flash magazine.

Case study

A 52-year-old woman underwent bilateral mastectomies and reconstructions for multifocal, ER+ bilateral breast cancer in 2010. 4 years later she re-presented with 6 months of bone pain while taking adjuvant Tamoxifen therapy. She was restaged with a whole-body MRI study for disease detection. A response assessment WB-MRI study was undertaken 14 weeks later, following 4 cycles of FEC chemotherapy and bisphosphonates (without growth factor support) (Figs. 1, 2). Unfortunately, 4 months later she developed intracranial metastatic disease and expired.

Continued on page 41.

Figure 2: Morphologic and diffusion-weighted images of the L2 vertebral body.

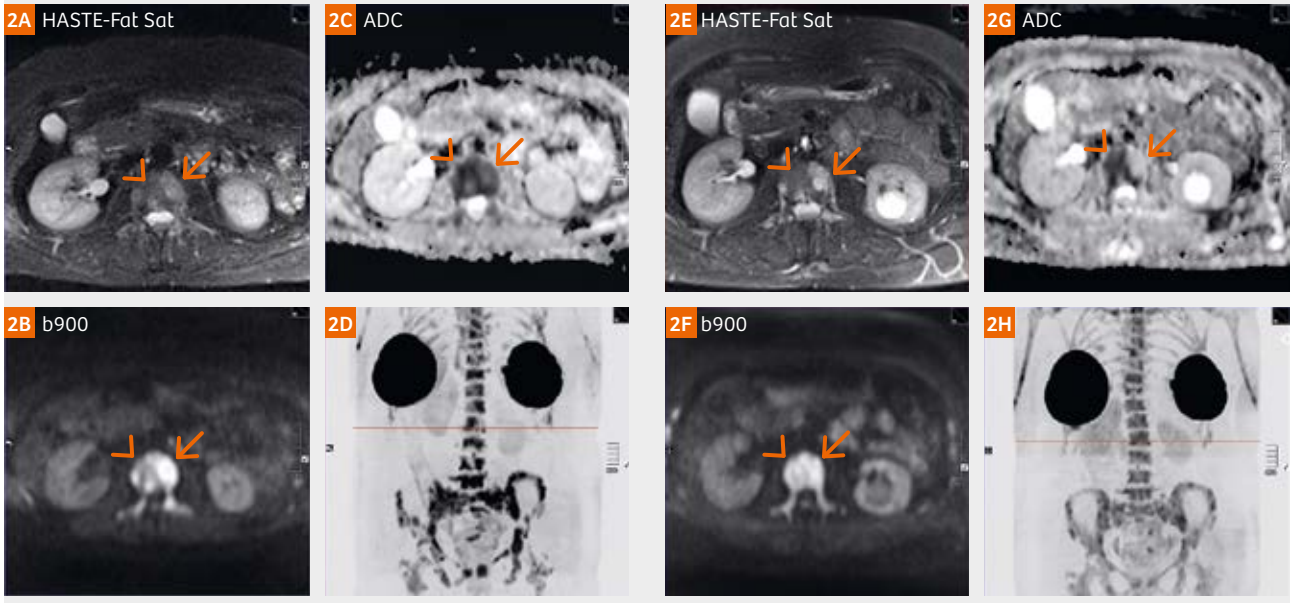

Axial HASTE-Fat Sat, b = 900 s/mm² and ADC images with zoomed whole-body b900 3D MIP (inverted scale) before and after therapy. Axial images are through the L2 vertebral body as indicated by the red reference line. The follow-up images (right 2 columns, **2E-H**) demonstrated excellent response to treatment, with increases in apparent diffusion coefficient (ADC) values for the metastatic deposit in the left side of the vertebral body (arrows). The bone marrow in the right side of the vertebral body (arrow head) demonstrates lowering of ADC values. In this area, the bone marrow T1w-fat percentage (F%) on corresponding Dixon images (not shown) changed from 20% to 26%.

Figure 3: Whole-body tumor load analysis.

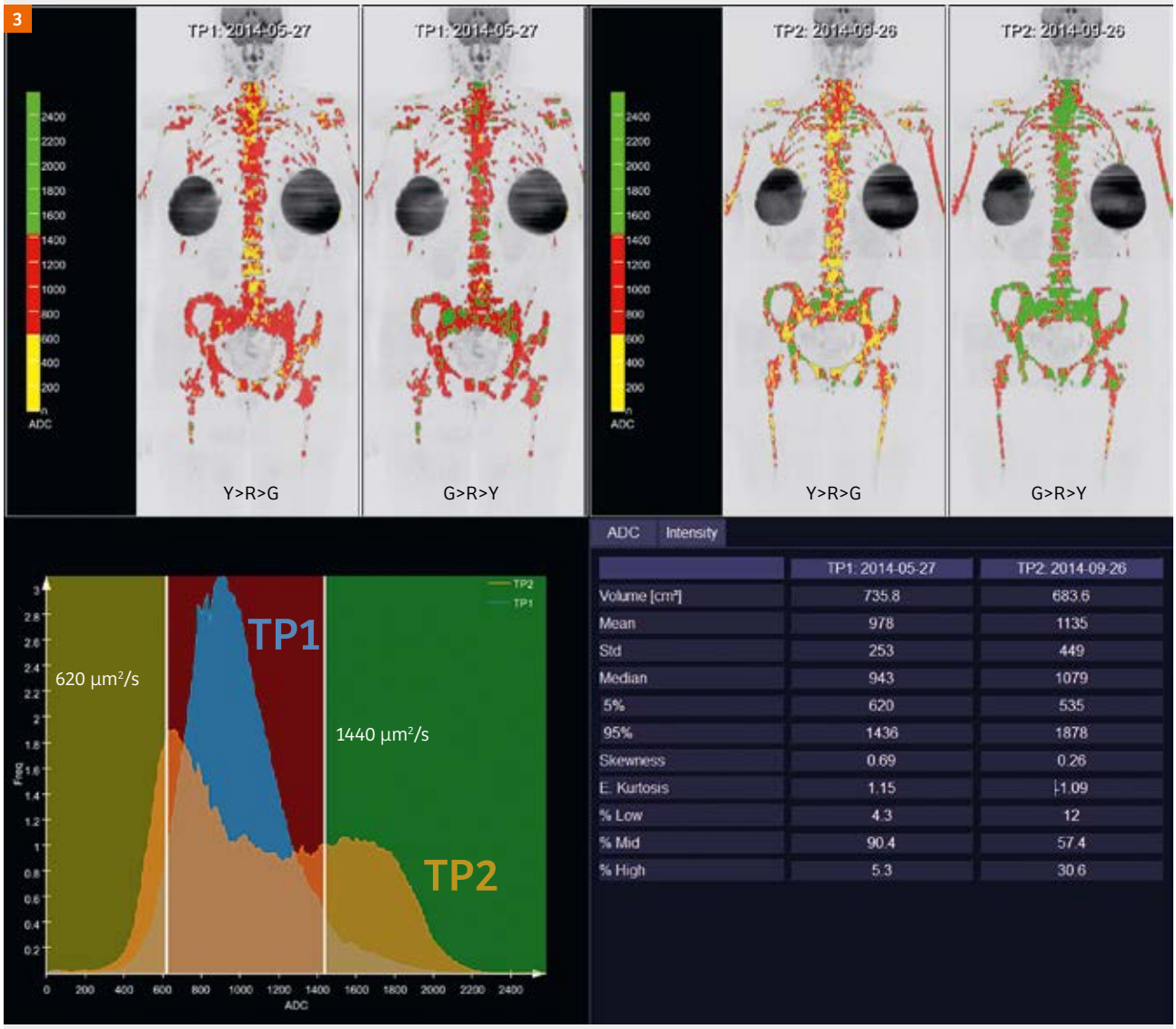

WB-tumor load segmentations were undertaken on *syngo.via* Frontier MR Total Tumor Load software[1] (Siemens Healthcare, released research prototype). The whole-body b900 images were segmented using computed high b-value images of 1000–1200 s/mm², setting a signal intensity threshold of approximately 30 AU. Extraneous signals (such as the brain, thyroid, kidneys, spleen, breast prostheses and bowel) were removed, to leave only recognizable bone sites. The b900 MIP images are overlaid with ADC value classes using the 5th and 95th centile values of the pre-treatment histogram (620 and 1440 µm²/s respectively). Red colored voxels represent untreated disease or those that have no-detected response. Green colored voxels have ADC values ≥ 1440 µm²/s (representing voxels that have increased in ADC values and are 'likely' to be responding). The yellow voxels lie below the 5th centile ADC value of the pre-treatment histogram (620 µm²/s). Thus, yellow voxels represent regions 'likely' to represent normal bone marrow.

736 mL of bone marrow was segmented before therapy and 684 mL after chemotherapy. Note that there is a global increase in median ADC values (943 µm²/s and 1079 µm²/s respectively), a decrease in excess kurtosis (1.15 and -1.1), and broadening of ADC histogram shown by an increase in the ADC standard deviation (253 and 449 µm²/s respectively), of the corresponding relative frequency histograms. There is unimodal distribution of ADC values before (TP1) and a bimodal distribution of the post-treatment (TP2) histogram. Note increasing numbers of yellow and green voxels representing normal bone marrow and cell kill respectively. There are also areas of red indicating residual active disease on TP2.

The color whole-body ADC class back-maps are of two types for each time point. On the left is the ADC color projection focusing on normal bone marrow (yellow voxels; MIP-ADC low image), and on the right of each pair is the ADC color projections focusing on response (green voxels; MIP-ADC high image).

The whole-body MRI scans with diffusion-weighted sequences were undertaken using a 1.5T MAGNETOM Avanto scanner using a published protocol [3]. The baseline scan (TP1) demonstrated extensive metastatic bone only disease (Figs. 1, 2) on morphological T1w and T2w-fs images of the spine.

The follow-up WB-MRI (TP2) demonstrated excellent response to treatment, with decreases in b = 900 s/mm² signal intensity and corresponding increases in apparent diffusion coefficient (ADC) values for individual metastatic deposits (Fig. 2 – arrows). Normal bone marrow return was also noted with increasing fat in the bone marrow (Fig. 2 – arrow heads).

The diffusion-weighted images for both examinations were analysed using threshold-based segmentation with *syngo*.via Frontier MR Total Tumour Load software[1] [7]. The pre-treatment ADC histogram has a unimodal distribution of ADC values (Fig. 3). After 4 cycles of chemotherapy, a bimodal distribution can be seen (Fig. 3). Increased voxels with high ADC values > 1500 µm²/s indicate the presence of tumor cell kill (arrows in Fig. 2). A new peak to the left of the pre-treatment ADC histogram represents the re-emergence of normal bone marrow (Fig. 3).

Discussion

The total tumor load software has been developed to enhance the value of ADC histogram analysis for assessing therapy response. The location of histogram ADC values is undertaken by color-coded projections of ADC classes on the b900 MIP images (MIP-ADC class pairing). In so doing, it is possible to anatomically localize the anatomic site and likely biologic state of the tissues. In this case example, normal bone marrow was assigned to ADC values that are lower than 620 µm²/s [10, 11] and displayed as yellow, voxels between 620 µm²/s and 1440 µm²/s are color coded as red (the 5th–95th centile values of the pre-treatment (TP1) ADC histogram), voxels with an ADC above 1440 µm²/s are shown in green, representing likely response.

The software, allows cycling through these color layers in order to focus the visualization on normal bone marrow (yellow), untreated active disease (red) or likely response (green), respectively (Fig. 4). Since only one color can be projected onto the segmented mask, the following rules are applied for the bone ADC color scheme (from lower to higher ADC values, Yellow-Red-Green).

ADC color projections focusing on marrow are shown on the left of each MIP-ADC class pair, if at least one voxel of the segmented bone has an ADC of less than 620 µm²/s, it will be assigned the yellow color (MIP-ADC low). Otherwise, it will be colored in red if any ADC is between 620 and 1440 µm²/s, or in green, if all ADC values along the projection are above 1440 µm²/s. Thus, the resulting projected color order for normal bone marrow is Yellow > Red > Green.

ADC color projections focusing on response are on the right of each image pair (MIP-ADC high). If at least one voxel of the segmented bone has an ADC of 1440 µm²/s or higher, it will be assigned a green color. Otherwise, it will be colored in red if the ADC falls between 620 and 1440 µm²/s, or in yellow, if all ADC values along the projection are below 620 µm²/s. Thus, the corresponding projected color order for assessing response is Green > Red > Yellow.

The use of ADC color projections, histograms and descriptive histogram statistics enables an easier to understand and objective method of assessing therapy response in bone marrow malignancies. When complex ADC changes occur simultaneously, as in this case (tumor response and bone marrow recovery), the ability to separate and visualize likely active disease, likely response and bone marrow recovery, can enable the success of treatment to be more effectively assessed. This is particularly useful when diffuse disease is present, when morphological images are often uninformative regarding the presence and extent of therapy response.

4

Color coding of ADC ranges:

Yellow (<620 µm²/s):	likely bone marrow
Red (620-1440 µm²/s):	likely untreated disease
Green (>1440 µm²/s):	likely response

(4A) Color projection focusing on normal bone marrow: Yellow voxels cover red and green voxels.

(4B) Color projection focusing on response: Green voxels cover red and yellow voxels.

Figure 4:
ADC color projection modes. In order for color projections to be able to preferentially visualize normal marrow or likely response, the color order for the ray tracing needs to be adjusted. For ADC color projections focusing on normal bone marrow **(4A)**, the ADC-MIP displays low ADC on top (ie, yellow). For ADC-MIP color projections focusing on response **(4B)**, the ADC-MIP displays high ADC on top (green). In this case the threshold for colors are derived from the pretherapy histogram.

[1] *syngo*.via Frontier is for research only, not a medical device. *syngo*.via Frontier MR Total Tumor Load is a released research prototype.

References

1 Woo, S., Suh, C. H., Kim, S. Y., Cho, J. Y., & Kim, S. H. (2017). Diagnostic Performance of Magnetic Resonance Imaging for the Detection of Bone Metastasis in Prostate Cancer: A Systematic Review and Meta-analysis. European Urology. doi:10.1016/j.eururo.2017.03.042.
2 Kosmin, M., Makris, A., Joshi, P. V., Ah-See, M., Woolf, D., & Padhani, A. R. (2017). The addition of whole-body magnetic resonance imaging to body computerised tomography alters treatment decisions in patients with metastatic breast cancer. European Journal of Cancer, 77, 109-116. doi:10.1016/j.ejca.2017.03.001.

Contact

Dr. Danoob Dalili
Specialist Registrar Clinical Radiology
Imperial College Healthcare NHS Trust
St Mary's Hospital
Praed St
London W2 1NY
United Kingdom
Phone: +44 (0) 20 3312 6666
Dalili@doctors.org.uk

Prof. Anwar R. Padhani
Consultant Radiologist and
Professor of Cancer Imaging
Paul Strickland Scanner Centre
Mount Vernon Cancer Centre
Rickmansworth Road
Northwood, Middlesex HA6 2RN
United Kingdom
Phone (PA): +44-(0) 1923-844751
Fax: +44-(0) 1923-844600
anwar.padhani@stricklandscanner.org.uk

3 Dimopoulos, M. A., Hillengass, J., Usmani, S., Zamagni, E., Lentzsch, S., Davies, F. E., & Terpos, E. (2015). Role of Magnetic Resonance Imaging in the Management of Patients With Multiple Myeloma: A Consensus Statement. Journal of Clinical Oncology, 33(6), 657-664. doi:10.1200/jco.2014.57.9961.
4 Padhani AR, Lecouvet FE, Tunariu N, et al. METastasis Reporting and Data System for Prostate Cancer (MET-RADS): Practical Guidelines for Acquisition, Interpretation, and Reporting of Whole-body MRI-based Evaluations of Multiorgan Involvement in Advanced Prostate Cancer. Eur Urol. 2017; 71(1):81-92.
5 Blackledge, M. D., Collins, D. J., Tunariu, N., Orton, M. R., Padhani, A. R., Leach, M. O., & Koh, D. (2014). Assessment of Treatment Response by Total Tumor Volume and Global Apparent Diffusion Coefficient Using Diffusion-Weighted MRI in Patients with Metastatic Bone Disease: A Feasibility Study. PLoS ONE, 9(4), e91779. doi:10.1371/journal.pone.0091779.
6 Blackledge, M. D., Tunariu, N., Orton, M. R., Padhani, A. R., Collins, D. J., Leach, M. O., & Koh, D. (2016). Inter- and Intra-Observer Repeatability of Quantitative Whole-Body, Diffusion-Weighted Imaging (WBDWI) in Metastatic Bone Disease. PLOS ONE, 11(4), e0153840. doi:10.1371/journal.pone.0153840.
7 Grimm R, Padhani AR. Whole-body Diffusion-weighted MR Image Analysis with *syngo.via* Frontier MR Total Tumor Load. MAGNETOM Flash (68) 2/2017, 73-75.
8 Padhani AR. Observing endocrine therapy resistance in metastatic breast cancer with whole body MRI. MAGNETOM Flash (68) 2/2017, 80-83.
9 Dalili D, Joshi P, Grimm R, Padhani AR. Evolution of the malignant bone marrow with successful therapy – quantitative analysis with whole body diffusion MRI. MAGNETOM Flash (69) 3/2017, 43–48.
10 Padhani, A. R., Van Ree, K., Collins, D. J., D'Sa, S., & Makris, A. (2013). Assessing the Relation Between Bone Marrow Signal Intensity and Apparent Diffusion Coefficient in Diffusion-Weighted MRI. American Journal of Roentgenology, 200(1), 163-170. doi:10.2214/ajr.11.8185.
11 Messiou C, Collins DJ, Morgan VA, Desouza NM. Optimising diffusion weighted MRI for imaging metastatic and myeloma bone disease and assessing reproducibility. Eur Radiol. 2011; 21(8):1713-8.

Watch Cancer Develop Multidrug Resistance

In this video Professor Padhani shows how quantitative whole-body MRI is used to monitor therapy response in metastatic breast cancer. Watch the video at

www.siemens.com/WB-MRI